

Unearthing the soil carbon food web with high resolution DNA-SIP

Ashley N Campbell and Charles Pepe-Ranney * † ‡, Chantal Koechli, Sean Berthrong, and Daniel H Buckley ‡

* These authors contributed equally to the manuscript and should be considered co-first authors, † Department of Microbiology, Cornell University, New York, USA, and ‡ Department of Crop and Soil Sciences, Cornell University, New York, USA

Submitted to Proceedings of the National Academy of Sciences of the United States of America

Abstract

We identified microorganisms participating in xylose and/or cellulose decomposition in soil microcosms using nucleic acid stable isotope probing (SIP) coupled to next generation sequencing. 49 and 63 OTUs assimilated ^{13}C from xylose and cellulose into DNA, respectively. Microorganisms assimilated xylose-C at days 1, 3, and 7. Cellulose-C assimilation peaked at day 14 and was maintained at day 30. Many SIP-identified cellulose degraders are members of cosmopolitan but physiologically uncharacterized soil microbial lineages including *Spartobacteria*, *Chloroflexi* and *Planctomycetes*. ^{13}C from Xylose was initially assimilated by *Firmicutes* followed by *Bacteroidetes* and *Actinobacteria*. Trophic interactions may have caused this temporal pattern. Soil C cycling models, however, often disregard bacterial trophic interactions. Fast growing substrate specialists assimilated xylose-C and slow growing substrate specialists assimilated cellulose-C. Cellulose-C assimilators within time points clustered phylogenetically, phylogenetically coherent groups assimilated xylose-C. Knowledge of soil C-cycling functional guild diversity and activity will improve the predictive power of terrestrial C flux models.

monolayer | structure | x-ray reflectivity | molecular electronics

Abbreviations: SAM, self-assembled monolayer; OTS, octadecyltrichlorosilane

Significance

We have a limited understanding of soil carbon (C) cycling yet soil contains a large fraction of the global C pool. Microorganisms mediate most soil C cycling but have proven difficult to study due to the complexity of soil C biochemistry and the wide range of soil microorganisms participating in C reactions. We demonstrate C use dynamics by soil microbial taxa. Furthermore, we identified microorganisms involved in cellulose, the most globally abundant biopolymer, decomposition that were previously uncharacterized physiologically. Our results expand knowledge of soil

functional guild diversity and activity which reveal soil function-structure relationships.

Introduction

Excluding plant biomass, there are 2,300 Pg of carbon (C) in soils worldwide which accounts for ~80% of the global terrestrial C pool [1, 2]. Fungi, archaea, and bacteria degrade plant biomass that reaches soil. Microorganisms respire the majority of plant biomass producing 10 times more CO_2 annually than anthropogenic emissions [3]. Rising atmospheric CO_2 may stimulate plant growth and in turn increase plant biomass C input to soil [4]. Current climate change models concur on atmospheric and oceanic, but not terrestrial, C predictions [5]. Contrasting terrestrial C model predictions reflect how little is known about soil C cycling. We must establish the roles and diversity of soil microbial community members in soil C cycling to reconcile inconsistencies in terrestrial C models [6, 7].

we must identify the *in situ* activity of soil microbes to establish soil structure function relationships [8]. Microorganisms mediate an estimated 80-90% of soil C cycling [9, 10]. The complexity of soil obscures microbial contributions to soil C cycling and the majority of microorganisms resist cultivation in the laboratory. Stable-isotope probing (SIP) links genetic identity and activity without cultivation and has expanded our knowledge of microbial contributions to biogeochemical processes [11]. Successful applications of SIP have identified organisms which me-

Reserved for Publication Footnotes

diate processes performed by functionally specialized microorganisms of limited diversity such as methanogens [12] but SIP has been less applicable in soil C cycling studies because simultaneous labeling of many different organisms required inhibitory resolving power. High throughput DNA sequencing technology, however, improves the resolving power of SIP enabling exploration of complex soil C-cycling patterns.

This study aimed to observe labile C versus polymeric C assimilation dynamics in the soil microbial community. We added mixture of nutrients and C substrates to soil microcosms that simulated the composition of plant biomass. All microcosms received the same C substrate mixture where the only difference between treatments was the identity of the isotopically labeled substrate. Specifically, we set up a series of microcosms with three treatments: in one treatment xylose was substituted for its ^{13}C -equivalent, in another cellulose was substituted for its ^{13}C -equivalent, and in the third treatment all substrates in the mixture were unlabeled. We harvested microcosms at days 1, 3, 7, 14 and 30 except day 1 where only ^{13}C -xylose treated microcosms were harvested. We used labeled xylose and cellulose to contrast labile C and polymeric C decomposition, respectively and we sequenced 16S rRNA genes from SIP density fractions with high throughput DNA sequencing technology. Our experimental design allowed us to observe the soil microbial community members that assimilated xylose-C and cellulose-C over time.

Results

Our experimental design allowed us to track the flow of xylose and cellulose C through the soil microbial community (Figure S1). 5.3 mg C substrate mixture per gram of soil was added to each microcosm representing 18% of the soil C. The mixture included 0.42 mg xylose-C and 0.88 mg cellulose-C per gram soil. Microcosms were harvested at days 1, 3, 7, 14 and 30 during a 30 day incubation. ^{13}C -xylose assimilation peaked immediately and tapered over the 30 day incubation whereas ^{13}C -cellulose assimilation peaked two weeks after amendment additions (Figure 1, Figure S2). See Supplemental Note XX for sequencing and density fractionation statistics. Microcosm treatments (see Methods) are identified in figures by the following code: “13CXPS” refers to the amendment with ^{13}C -xylose (^{13}C Xylose Plant Simulant), “13CCPS” refers to the ^{13}C -cellulose amendment and “12CCPS” refers to the amendment that only contained ^{12}C (i.e. control).

Soil microcosm microbial community changes with time. Changes in the bulk soil microcosm microbial community structure and membership cor-

related significantly with time (Figure S3, p-value 0.23, R^2 0.63, Adonis test [13]). The identity of the ^{13}C -labeled substrate added to the microcosms did not significantly correlate with bulk soil community structure and membership (p-value 0.35). Additionally, microcosm beta diversity was significantly less than gradient fraction beta diversity (Figure S3, p-value 0.003, “betadisper” function R Vegan package [14, 15]). Twenty-nine OTUs significantly changed in relative abundance with time (“BH” adjusted p-value <0.10, [16]) and of these 29 OTUs, 14 were found to incorporate ^{13}C from labeled substrates into biomass (Figure S4). Four taxonomic classes significantly (adjusted P-value ≤ 0.10) changed in abundance: *Bacilli* (decreased), *Flavobacteria* (decreased), *Gammaproteobacteria* (decreased) and *Herpetosiphonales* (increased) (Figure S5). Abundances grouped by phylum for OTUs that incorporated ^{13}C from cellulose increased with time whereas abundances grouped by phylum of OTUs that incorporated ^{13}C from xylose decreased over time although *Proteobacteria* abundance spiked at day 14 (Figure S6).

OTUs that assimilated ^{13}C into DNA. Within the first 7 days of incubation 63% of ^{13}C -xylose was respired and only 6% more was respired from day 7 to 30. At day 30, 30% of the ^{13}C from xylose remained in the soil. An average 16% of the ^{13}C -cellulose added was respired within the first 7 days, 38% by day 14, and 60% by day 30.

We refer to OTUs that putatively incorporated ^{13}C into DNA originally from an isotopically labeled substrate as substrate “responders” (see Supplemental Note XX for operational “response” criteria). There were 19, 19, 15, 6, and 1 ^{13}C -xylose responders at days 1, 3, 7, 14, 30, respectively (Figure S2). The numerically dominant ^{13}C -xylose responder phylum shifted from *Firmicutes* to *Bacteroidetes* and then to *Actinobacteria* across days 1, 3 and 7 (Figure 2, Figure 3). *Proteobacteria* ^{13}C -xylose responders were found at days 1, 3, 7 but peaked at day 7 (Figure 3).

Only 2 and 5 OTUs responded ^{13}C -cellulose at days 3 and 7, respectively. At days 14 and 30, 42 and 39 OTUs responded to ^{13}C -cellulose. (Figure S2). *Proteobacteria*, *Verrucomicrobia*, and *Chloroflexi* had relatively high numbers of responders with strong response across multiple time points (Figure 2). *Verrucomicrobia* ^{13}C -cellulose responders were 70% *Spartobacteria*. *Chloroflexi* responders were annotated belonging to the *Herpetosiphonales* and *Anaerolineae* (Figure ??). *Celvibrio*, a canonical soil cellulose degrader, was found to respond strongly in the microcosms to ^{13}C -cellulose. See Supplemental Note XX for further counts of ^{13}C -responsive OTUs at greater taxonomic resolution.

¹⁹⁵ **Ecological strategies of ¹³C responders.** ¹³C-xylose responders are generally more abundant members based on relative abundance in bulk DNA SSU rRNA gene content than ¹³C-cellulose responders (Figure 4, p-value 0.00028, Wilcoxon Rank Sum test). However, both abundant and rare OTUs responded to ¹³C-xylose and ¹³C-cellulose (Figure 4). Two ¹³C-cellulose responders were not found in any bulk samples (“OTU.862” and “OTU.1312”, Table S1). Of the 10 most abundant ²⁰⁵ responders, 8 are ¹³C-xylose responders and 6 of these 8 are consistently among the 10 most abundant OTUs in bulk samples.

Cellulose responder buoyant density (BD) shifted further along the density gradient than ²¹⁰ xylose responder BD in response to ¹³C incorporation (Figure S7, Figure 4, p-value 1.8610⁻⁰⁶, Wilcoxon Rank Sum test). ¹³C-cellulose responder BD shifted on average 0.0163 g mL⁻¹ (sd 0.0094) whereas xylose responder BD shifted on average ²¹⁵ 0.0097 g mL⁻¹ (sd 0.0094). For reference, 100% ¹³C DNA BD is 0.04 g mL⁻¹ greater than the BD of its ¹²C counterpart. DNA BD increases as its ratio of ¹³C to ¹²C increases. An organism that ²²⁰ only assimilates C into DNA from a ¹³C isotopically labeled source, will have a greater ¹³C to ¹²C ratio in its DNA than an organism utilizing a mixture of isotopically labeled and unlabeled C sources (see Supplemental Note XX). We predicted the *rrn* gene copy number for each OTU as described previously [17]. The estimated *rrn* gene copy number for ¹³C-xylose responders was inversely related to time point of the first response per OTU (p-value 2.02x10⁻¹⁵, Figure S8). OTUs that did not respond at day 1 respond but did respond at day 3 ²²⁵ and/or day 7 had fewer estimated *rrn* copy number than OTUs that responded at day 1 (Figure S8).

We assessed phylogenetic clustering of ¹³C-responsive OTUs with the Nearest Taxon Index (NTI) and the Net Relatedness Index (NRI). ²³⁰ Briefly, positive NRI and NTI with corresponding low P-values indicates deep phylogenetic clustering whereas negative NRI with high P-values indicates taxa are overdispersed compared to the null model [18]. NRI and P-values for substrate responder groups suggest ¹³C-xylose responders are overdispersed (NRI: -1.33, P: 0.90) while ¹³C-cellulose responders are clustered (NRI: 4.49, P: 0.001). NTI values show that both ¹³C-cellulose and ¹³C-xylose ²⁴⁰ responders are clustered near the tips of the tree (NTI: 1.43 (P: 0.072), 2.69 (P: 0.001), respectively).

Discussion

Microbial response to isotopic labels. DNA-SIP can establish functional roles for thousands of phylogenetic types in a single experiment without cultivation. ²⁵⁰

We identified 104 soil OTUs that incorporated ¹³C from xylose and/or cellulose into biomass and characterized substrate specificity and C-cycling dynamics for these OTUs. We propose xylose and cellulose C added to soil microcosms took the following path through the microbial food web (Figure S9): fast-growing *Firmicutes* spore formers first assimilated labile C followed by *Bacteroidetes*, *Actinobacteria* and *Proteobacteria* phylotypes. The *Bacteroidetes*, *Actinobacteria* and *Proteobacteria* phylotypes may have also preyed on the rapidly responding *Firmicutes*. Canonical cellulose degrading bacteria such as *Cellvibrio* and members of cosmopolitan yet functionally uncharacterized soil phylogenetic groups like *Chloroflexi*, *Planctomycetes* and *Verrucomicrobia*, specifically the *Spartobacter*, decomposed cellulose. Cellulose C incorporation into microbial biomass peaked at day 14 and was maintained through day 30.

Ecological strategies of soil microorganisms participating in the decomposition of organic matter. We assessed ¹³C-responsive OTU ecological strategies by estimating each OTU's *rrn* gene copy number and BD shift due to ¹³C-labeling. *rrn* gene copy number correlates positively with, and indicates, growth rate [17, 19], whereas BD shift indicates substrate specificity (see Results). ²⁷⁰ ¹³C-cellulose responsive OTUs grow slower (Figure 4, Figure S8), have greater substrate specificity (Figure 4), and are generally lower abundance members of the bulk community than ¹³C-xylose responsive OTUs (Figure 4). High *rrn* gene copy number may inflate ¹³C-xylose-responder abundance. ²⁷⁵ ¹³C-xylose responsive OTUs that incorporate ¹³C into biomass at day one had greater *rrn* gene copy number than OTUs that responded later (Figure 4, Figure S8) suggesting fast-growing microbes assimilated ¹³C from xylose before slow growers.

NRI values quantify phylogenetic clustering [20] ²⁹⁰ and have been used to assess clustering of soil OTUs that responded similarly to soil wet up [18, 21]. To our knowledge, assessing phylogenetic clustering of OTUs found to incorporate heavy isotopes into biomass during SIP incubations has not been attempted. We found that ¹³C-cellulose and xylose responders are clustered and overdispersed, respectively. This suggests that the ability to degrade cellulose is phylogenetically conserved possibly reflecting the complexity of cellulose degradation biochemistry. The positive relationship between a physiological trait's phylogenetic depth and complexity has been noted previously [22] and the clustering depth of ¹³C-cellulose responders, X.XX 16S rRNA gene sequence divergence, is on the same order as that observed for glycoside hydrolases which are diagnostic enzymes for cellulose degradation [23]. Overdispersion, as we saw for

the ^{13}C -xylose responsive OTUs, may be indicative of a readily horizontally transferred trait and/or a trait that is broadly distributed phylogenetically, or, in this case may indicate that the group comprises more than one trait. It's not clear which ^{13}C -xylose responsive organisms were labeled as a result of primary xylose assimilation (see below), and therefore it's not clear if ^{13}C -xylose responsive OTUs in this experiment constitute a single ecologically meaningful group or multiple ecological groups. Temporally defined ^{13}C -xylose responder groups, however, are phylogenetically coherent (Figure ??, Figure 3). For example, most day 1 ^{13}C -xylose responders are members of the *Paenibacillus* (see Supplemental Note XX).

Intuitively we infer C cycling functional guild diversity from the distribution of diagnostic genes across genomes CITE or from screening culture collections for a particular trait CITE. For instance, the wide distribution of the glycolysis operon in microbial genomes is interpreted as evidence that many soil microorganisms participate in glucose turnover CITE. *In situ* functional guild diversity, however, can vary significantly from diversity assessed by functionally screening isolates and/or genomes. Xylose use in soil, for instance, may be less a function of catabolic pathway distribution among genomes and more a function of lifestyle. Seasonal change CITE, land management CITE, and rainfall CITE pulse deliver nutrients and resources to soil. Therefore, fast growth and/or rapid resuscitation upon wet up CITE allow microorganisms to favorably compete for labile C resources. Life history determines growth rate and dessication resistance whereas the ability to use labile C is phylogenetically dispersed so life history may constrain the diversity of labile C assemblers. DNA-SIP is useful for establishing *in situ* phylogenetic clustering and diversity of functional guilds because DNA-SIP can account for life history strategies by targeting active microorganisms. Additionally, snapshot estimates of community composition commonly inform soil structure-function-relationship studies CITE Fierer but labile C decomposition might not be linked to snapshot community structure, but alternatively to community structure dynamics. Fast growing spore formers would not need to maintain high abundance to significantly mediate cycling of pulse delivered resources. This accentuates the usefulness of DNA-SIP for describing soil ecology as DNA-SIP assesses activity which can be decoupled from snapshot abundance.

Need to incorporate Fierer 2007 paper
Paenibacillus Neufeld
 Thompson “all bands enriched”

Implications for soil C cycling models. Land management, climate, pollution and disturbance can influence soil community composition [24] which in turn influences soil biogeochemical process rates (e.g. [25]). Assessing functional group diversity and establishing identities of functional group members is necessary to predict how biogeochemical process rates will change with community composition [24, 26]. Aggregate biogeochemical processes that are the sum of many subprocesses involve a broad array of taxa and are assumed to be less influenced by community change than narrow processes that involve a single, specific chemical transformation by a smaller suite of microbial participants [24, 26]. Within an aggregate process such as C decomposition, subprocesses can be further classified as broad or narrow [24]. In theory, “broad” and “narrow” functional guilds decompose labile and recalcitrant C, respectively [24]. However, the diversity of active labile C and insoluble, polymeric C decomposers in soil has not been directly quantified. Notably, we found more OTUs responded to ^{13}C -cellulose, 63, than ^{13}C -xylose, 49. Also, it is possible that many ^{13}C -xylose responders are predatory bacteria as opposed to primary labile C degraders (see below). Cellulose and xylose decomposer functional guilds were non-overlapping in membership – of 104 ^{13}C -responders only 8 responded to both cellulose and xylose – and represented a small fraction of total soil community diversity (Figure 5). While xylose use is undoubtedly more widely distributed among microbial genomes than the ability to degrade cellulose, active cellulose decomposers outnumbered active xylose utilizers.

Both ^{13}C -cellulose and ^{13}C -xylose responders largely clustered near the tips of the phylogenetic tree ($\text{NTI} > 0$) at taxonomic levels broader than the OTUs established in this study (Figure S10). Therefore, ^{13}C -responders distribute into fewer clades than OTUs (Figure S10). ^{13}C -xylose responders formed clades at X.XX sequence divergence (consenTrait) while our OTUs were established at 0.03 sequence divergence.

Trophic interactions or the functional groups tuned to different resource concentrations caused the activity succession from *Firmicutes* to *Bacteroidetes* and finally *Actinobacteria* in response to xylose addition. *Actinobacteria* (e.g. *Agromyces*) and *Bacteroidetes* have been previously implicated as predatory soil bacteria [27, 28], and, *Bacteroidetes* and *Actinobacteria* activity peaked while *Firmicutes* ^{13}C -xylose responder relative abundance decreased in our microcosms. Considering *Agromyces* and *Bacteroidetes* phylotypes are likely soil predators, one parsimonious hypothesis for ^{13}C -labelling of *Bacteroidetes* and *Actinobacteria* with a corresponding decrease ^{13}C -labeled

Firmicutes abundance is that *Bacteroidetes* and *Actinobacteria* fed on ^{13}C -labeled *Firmicutes*. If the temporal dynamics of ^{13}C -xylose incorporation are due to trophic interactions predatory bacteria consumed, many, if not most, fast-growing labile C degraders. Hence, soil C cycling models should include predatory interactions between soil bacteria but rarely do (e.g. [29]).

We propose two scenarios in the context of our results whereby community composition could affect C dynamics and fate. Genomic evidence shows cellulose degradation is a phylogenetically conserved trait CITE Allison. Our study evaluates the phylogenetic conservation of soil cellulose degradation in active microorganisms via DNA-SIP and genomic evidence concurs with our results. A decrease in cellulose degraders abundance would diminish cellulose decomposition process rates as few soil microorganisms can fill the phylogenetically conserved cellulose degradation niche. Dispersed cellulose decomposers could renew ecosystem function, however. For labile C decomposition, the absence fast growing spore formers would allow other microbes to assimilate labile C provided dispersal does not enable rapid recolonization CITE. Primary labile C degraders in this study grow fast, and form spores and these distinct ecological strategies might indicate distinct C use dynamics and/or resource allocation. New labile C degraders may metabolize and allocate labile C differently thus changing labile C dynamics and fate. Further, labile C degrader substitution could affect biomass C turnover by predatory bacteria that feed on fast growing, spore forming labile C decomposers. On the other hand, spore formation enables dispersal which would allow fast growing spore formers to continuously occupy the labile C decomposition niche CITE. One proposed mechanism for similar decomposition rates of labile C across soils varying in community composition is that labile C can be used widely by microorganisms CITE. An alternative hypothesis for consistent labile C process rates across different soils is that labile C degraders disperse readily. Notably, other lineages implicated in rapid labile C turnover include members of the *Actinobacteria* CITE Placella and many soil *Actinobacteria* form hyphae that facilitate dispersal CITE. The two hypotheses are not mutually exclusive, but our results suggest that environmental conditions unfavorable to fast-growing spore-formers and/or quickly resuscitated, hyphal *Actinobacteria* CITE may impact labile C dynamics and fate.

Conclusion. Microorganisms sequester atmospheric C and respire SOM influencing climate change on a global scale but we do not know which microorganisms carry out specific soil C transforma-

tions. In this experiment microbes from physiologically uncharacterized but ubiquitous soil lineages participated in cellulose decomposition. Cellulose C degraders included members of the *Verrucomicrobia* (*Spartobacteria*), *Chloroflexi*, *Bacteroidetes* and *Planctomycetes*. *Spartobacteria* in particular are globally cosmopolitan soil microorganisms and are often the most abundant *Verrucomicrobia* order in soil [30]. Fast-growing *Firmicutes* spore formers assimilated labile C in our microcosms. *Bacteroidetes* and *Actinobacteria* phylotypes, previously implicated as predators, may have fed on the fast growing *Firmicutes*. Our results suggest that, cosmopolitan *Spartobacteria* may degrade cellulose on a global scale, bacterial tropic interactions can significantly impact soil C cycling, and life history constrains functional guild diversity for labile C decomposition.

Methods

Additional information on sample collection and analytical methods is provided in SI Materials and Methods.

Twelve soil cores (5 cm diameter x 10 cm depth) were collected from six random sampling locations within an organically managed agricultural field in Penn Yan, New York. Soils were pretreated by sieving (2 mm), homogenizing sieved soil, and pre-incubating 10 g of dry soil weight in flasks for 2 weeks. Soils were amended with a 5.3 mg g soil⁻¹ carbon mixture; representative of natural concentrations [31]. Mixture contained 38% cellulose, 23% lignin, 20% xylose, 3% arabinose, 1% galactose, 1% glucose, and 0.5% mannose by mass, with the remaining 13.5% mass composed of an amino acid (in-house made replica of Teknova C0705) and basal salt mixture (Murashige and Skoog, Sigma Aldrich M5524). Three parallel treatments were performed; (1) unlabeled control, (2) ^{13}C -cellulose, (3) ^{13}C -xylose (98 atom% ^{13}C , Sigma Aldrich). Each treatment had 2 replicates per time point (n = 4) except day 30 which had 4 replicates; total microcosms per treatment n = 12, except ^{13}C -cellulose which was not sampled at day 1, n = 10. Other details relating to substrate addition can be found in SI. Microcosms were sampled destructively (stored at -80°C until nucleic acid processing) at days 1 (control and xylose only), 3, 7, 14, and 30.

Nucleic acids were extracted using a modified Griffiths protocol [32]. To prepare nucleic acid extracts for isopycnic centrifugation as previously described [33], DNA was size selected (>4kb) using 1% low melt agarose gel and β -agarase I enzyme extraction per manufacturers protocol (New England Biolab, M0392S). For each time point in the series isopycnic gradients were setup using a modi-

535 fied protocol [34] for a total of five ^{12}C -control, five ^{13}C -xylose, and four ^{13}C -cellulose microcosms. A
 536 density gradient (average density 1.69 g mL^{-1}) solution of $1.762 \text{ g cesium chloride (CsCl) ml}^{-1}$ in
 537 gradient buffer solution (pH 8.0 15 mM Tris-HCl,
 538 15 mM EDTA, 15 mM KCl) was used to separate
 539 ^{13}C -enriched and ^{12}C -nonenriched DNA. Each
 540 gradient was loaded with approximately $5 \mu\text{g}$ of
 541 DNA and ultracentrifuged for 66 h at 55,000 rpm
 542 and room temperature (RT). Fractions of $\sim 100 \mu\text{L}$
 543 were collected from below by displacing the DNA-
 544 CsCl-gradient buffer solution in the centrifugation
 545 tube with water using a syringe pump at a flow
 546 rate of $3.3 \mu\text{L s}^{-1}$ [35] into AcroprepTM 96 filter
 547 plate (Pall Life Sciences 5035). The refractive in-
 548 dex of each fraction was measured using a Reichart
 549 AR200 digital refractometer modified as previously
 550 described [33] to measure a volume of $5 \mu\text{L}$. Then
 551 buoyant density was calculated from the refractive
 552 index as previously described [33] (see also SI). The
 553 collected DNA fractions were purified by repetitive
 554 washing of Acroprep filter wells with TE. Finally,
 555 50 μL TE was added to each fraction then resus-
 556 pended DNA was pipetted off the filter into a new
 557 microfuge tube.
 558 For every gradient, 20 fractions were chosen for
 559 sequencing between the density range $1.67\text{--}1.75 \text{ g mL}^{-1}$. Barcoded 454 primers were designed using
 560 454-specific adapter B, 10 bp barcodes [36], a 2
 561 bp linker (5'-CA-3'), and 806R primer for reverse
 562 primer (BA806R); and 454-specific adapter A, a 2
 563 bp linker (5'-TC-3'), and 515F primer for for-
 564 ward primer (BA515F). Each fraction was PCR
 565 amplified using $0.25 \mu\text{L}$ 5 U μl^{-1} AmpliTaq Gold
 566 (Life Technologies, Grand Island, NY; N8080243),
 567 2.5 μL 10X Buffer II (100 mM Tris-HCl, pH 8.3,
 568 500 mM KCl), 2.5 μL 25 mM MgCl₂, 4 μL 5
 569 mM dNTP, 1.25 μL 10 mg mL^{-1} BSA, 0.5 μL
 570 10 μM BA515F, 1 μL 5 μM BA806R, 3 μL H₂O,
 571 10 μL 1:30 DNA template) in triplicate. Samples
 572 were normalized either using Pico green quantifica-
 573 tion and manual calculation or by SequalPrepTM
 574 normalization plates (Invitrogen, Carlsbad, CA;
 575 A10510), then pooled in equimolar concentrations.
 576 Pooled DNA was gel extracted from a 1% agarose
 577 gel using Wizard SV gel and PCR clean-up sys-
 578 tem (Promega, Madison, WI; A9281) per man-
 579 ufacturer's protocol. Amplicons were sequenced
 580 on Roche 454 FLX system using titanium chem-
 581 istry at Selah Genomics (formerly EnGenCore,
 582 Columbia, SC)

References

1. Amundson R (2001) The carbon budget in soils. *Annu Rev Earth Planet Sci* 29(1): 535–562.
2. Batjes N-H (1996) Total carbon and nitrogen in the soils of the world. *European Journal of Soil Science* 47(2): 151–163.
3. Chapin F (2002) Principles of terrestrial ecosystem ecology.
4. Groenigen K-J, Graaff M-A, Six J, Harris D, Kuikman P, Kessel C (2006) The impact of elevated atmospheric CO₂ on soil C and N dynamics: a meta-analysis. *Managed Ecosystems and CO₂* (Springer Science, Berlin Heidelberg), pp 373–391.
5. Friedlingstein P, Cox P, Betts R, Bopp L, von W-B, Brovkin V, et al. (2006) Climate–carbon cycle feedback analysis: Results from the C4 model intercomparison. *J Climate* 19(14): 3337–3353.
6. Neff J-C, Asner G-P (2001) Dissolved organic carbon in terrestrial ecosystems: synthesis and a model. *Ecosystems* 4(1): 29–48.
7. Warning: citation key “McGuire2010a” is not in the bibliography database.
8. O'Donnell A-G, Seasman M, Macrae A, Waite I, Davies J-T (2002) Plants and fertilisers as drivers of change in microbial community structure and function in soils. *Interactions in the Root Environment: An Integrated Approach* (Springer, Netherlands), pp 135–145.
9. Coleman D-C, Crossley D-A (1996) Fundamentals of Soil Ecology.
10. Nannipieri P, Ascher J, Ceccherini M-T, Landi L, Pietramellara G, Renella G (2003) Microbial diversity and soil functions. *European Journal of Soil Science* 54(4): 655–670.
11. Chen Y, Murrell J-C (2010) When metagenomics meets stable-isotope probing: progress and perspectives. *Trends Microbiol* 18(4): 157–163.
12. Lu Y (2005) In situ stable isotope probing of methanogenic archaea in the rice rhizosphere. *Science* 309(5737): 1088–1090.
13. Anderson M-J (2001) A new method for non-parametric multivariate analysis of variance. *Austral Ecology* 26(1): 32–46.
14. Anderson M-J, Ellingsen K-E, McArdle B-H (2006) Multivariate dispersion as a measure of beta diversity. *Ecology Letters* 9(6): 683–693.
15. Oksanen J, Kindt R, Legendre P, OHara B, Stevens M-HH, Oksanen M-J, et al. (2007) The vegan package.
16. Benjamini Y, Hochberg Y (1995) Controlling the false discovery rate: a practical and powerful approach to multiple testing. *Journal of the Royal Statistical Society, Series B* 57(1): 289–300.
17. Kembel S-W, Wu M, Eisen J-A, Green J-L (2012) Incorporating 16S gene copy number information improves estimates of microbial diversity and abundance. *PLoS Comput Biol*

- 8(10): e1002743.
18. Evans S-E, Wallenstein M-D (2014) Climate change alters ecological strategies of soil bacteria. *Ecol Lett* 17(2): 155–164.
19. Klappenbach J, Saxman P, Cole J, Schmidt T (2001) rrndb: the Ribosomal RNA Operon Copy Number Database.. *Nucleic Acids Res* 29(1): 181–184.
20. Webb C-O (2000) Exploring the phylogenetic structure of ecological communities: an example for rain forest trees.. *The American Naturalist* 156(2): 145–155.
21. Placella S-A, Brodie E-L, Firestone M-K (2012) Rainfall-induced carbon dioxide pulses result from sequential resuscitation of phylogenetically clustered microbial groups. *PNAS* 109(27): 10931–10936.
22. Martiny A-C, Treseder K, Pusch G (2013) Phylogenetic conservatism of functional traits in microorganisms. *ISMEJ* 7(4): 830–838.
23. Berlemont R, Martiny A-C (???) Phylogenetic distribution of potential cellulases in bacteria. *Appl Environ Microbiol* 79(5): 1545–1554.
24. McGuire K-L, Treseder K-K (2010) Microbial communities and their relevance for ecosystem models: Decomposition as a case study. *Soil Biology and Biochemistry* 42(4): 529–535.
25. Berlemont R, Allison S-D, Weihe C, Lu Y, Brodie E-L, Martiny J-BH, et al. (2014) Cellulolytic potential under environmental changes in microbial communities from grassland litter. *Front Microbiol* 5: 639.
26. Schimel J (1995) Ecosystem consequences of microbial diversity and community structure. *Arctic and alpine biodiversity: patterns, causes and ecosystem consequences*, , eds. III P-DFSC, Körner P-DC, Ecological Studies (Springer, Berlin Heidelberg), pp 239–254.
27. Lueders T, Kindler R, Miltner A, Friedrich M-W, Kaestner M (2006) Identification of bacterial micropredators distinctively active in a soil microbial food web. *Appl Environ Microbiol* 72(8): 5342–5348.
28. Casida L-E (1983) Interaction of Agromyces ramosus with Other Bacteria in Soil.. *Appl Environ Microbiol* 46(4): 881–888.
29. Moore J-C, Walter D-E, Hunt H-W (1988) Arthropod Regulation of Micro- and Mesobiota in Below-Ground Detrital Food Webs. *Annu Rev Entomol* 33(1): 419–435.
30. Bergmann G-T, Bates S-T, Eilers K-G, Lauber C-L, Caporaso J-G, Walters W-A, et al. (2011) The under-recognized dominance of Verrucomicrobia in soil bacterial communities. *Soil Biology and Biochemistry* 43(7): 1450–1455.
31. Schneckenberger K, Demin D, Stahr K, Kuzyakov Y (2008) Microbial utilization and mineralization of ^{14}C glucose added in six orders of concentration to soil. *Soil Biology and Biochemistry* 40(8): 1981–1988.
32. Griffiths R-I, Whiteley A-S, O'Donnell A-G, Bailey M-J (2000) Rapid method for coextraction of DNA and RNA from natural environments for analysis of ribosomal DNA- and rRNA-based microbial community composition. *Appl Environ Microbiol* 66(12): 5488–5491.
33. Buckley D-H, Huangyutitham V, Hsu S-F, Nelson T-A (2007) Stable isotope probing with ^{15}N achieved by disentangling the effects of genome G+C content and isotope enrichment on dna Density. *Appl Environ Microbiol* 73(10): 3189–3195.
34. Neufeld J-D, Vohra J, Dumont M-G, Lueders T, Manefield M, Friedrich M-W, et al. (2007) DNA stable-isotope probing. *Nature Protocols* 2(4): 860–866.
35. Manefield M, Whiteley A-S, Griffiths R-I, Bailey M-J (2002) RNA Stable isotope probing a novel means of linking microbial community function to phylogeny. *Appl Environ Microbiol* 68(11): 5367–5373.
36. Hamady M, Walker J-J, Harris J-K, Gold N-J, Knight R (2008) Error-correcting barcoded primers for pyrosequencing hundreds of samples in multiplex. *Nat Meth* 5(3): 235–237.

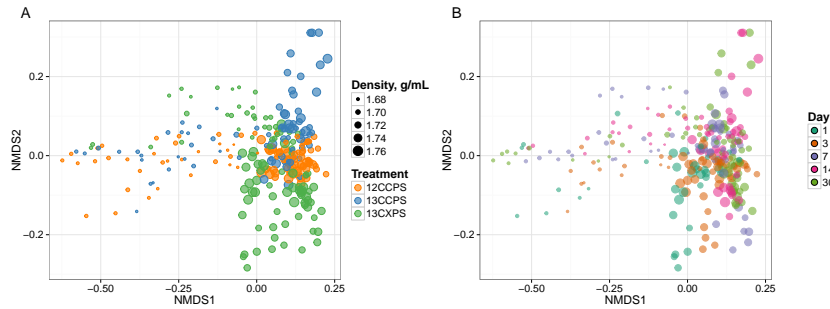


Fig. 1. NMDS analysis from weighted unifrac distances of 454 sequence data from SIP fractions of each treatment over time. Twenty fractions from a CsCl gradient fractionation for each treatment at each time point were sequenced (Fig. S1). Each point on the NMDS represents the bacterial composition based on 16S sequencing for a single fraction where the size of the point is representative of the density of that fraction and the colors represent the treatments (A) or days (B).

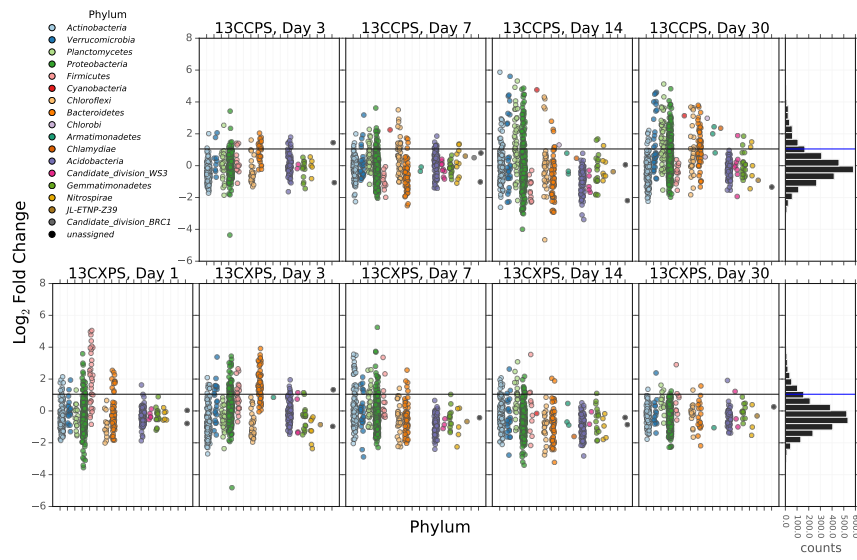


Fig. 2. Log₂ fold change of ¹³C-responders in cellulose treatment (top) and xylose treatment (bottom). Log₂ fold change is based on the relative abundance in the experimental treatment compared to the control within the density range 1.7125–1.755 g ml⁻¹. Taxa are colored by phylum. ‘Counts’ is a histogram of log₂ fold change values.

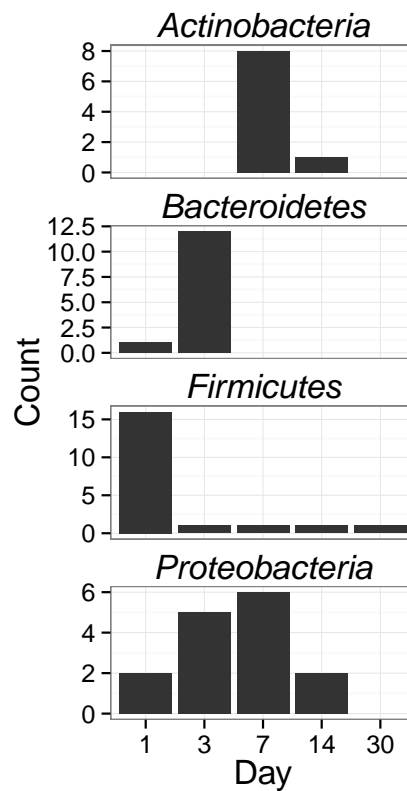


Fig. 3. Counts of ^{13}C -xylose responders in the *Actinobacteria*, *Bacteroidetes*, *Firmicutes* and *Proteobacteria* at days 1, 3, 7 and 30.

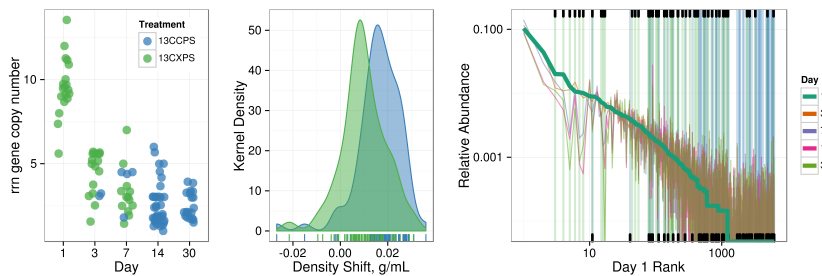


Fig. 4. ^{13}C -responder characteristics based on density shift (A) and rank (B). Kernel density estimation of ^{13}C -responder's density shift in cellulose treatment (blue) and xylose treatment (green) demonstrates degree of labeling for responders for each respective substrate. ^{13}C -responders in rank abundance are labeled by substrate (cellulose, blue; xylose, green). Ticks at top indicate location of ^{13}C -xylose responders in bulk community. Ticks at bottom indicate location of ^{13}C -cellulose responders in bulk community. OTU rank was assessed from day 1 bulk samples.

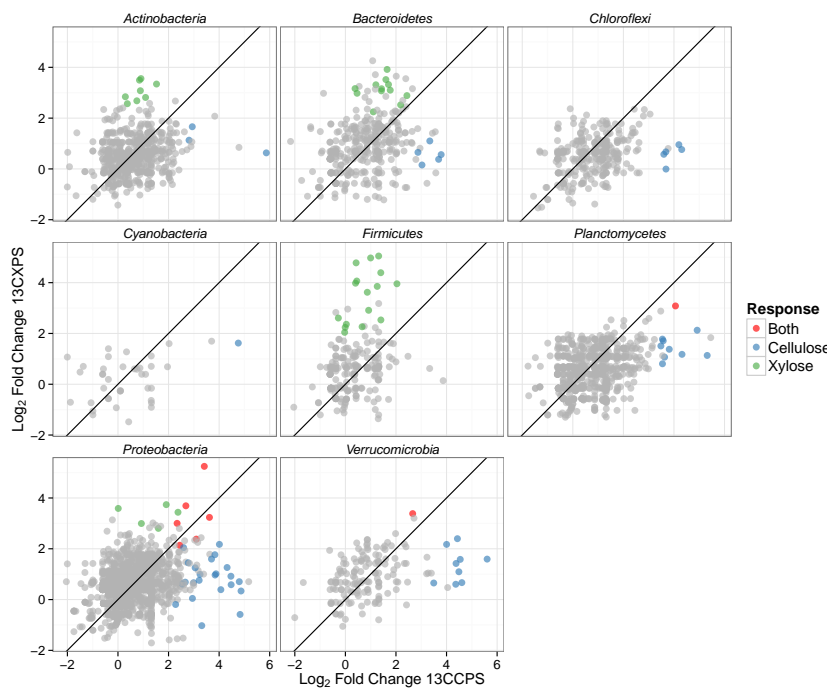


Fig. 5. Maximum log₂ fold change in response to labeled substrate incorporation for each substrate and all OTUs that pass sparsity filtering in both substrate analyses. Points colored by response. Line has slope of 1 with intercept at the origin. OTUs falling in the top-right quadrant responded to both substrates while those in the top-left and bottom-right responded to ¹³C-xylose and ¹³C-cellulose, respectively.

Supplemental Figures and Tables

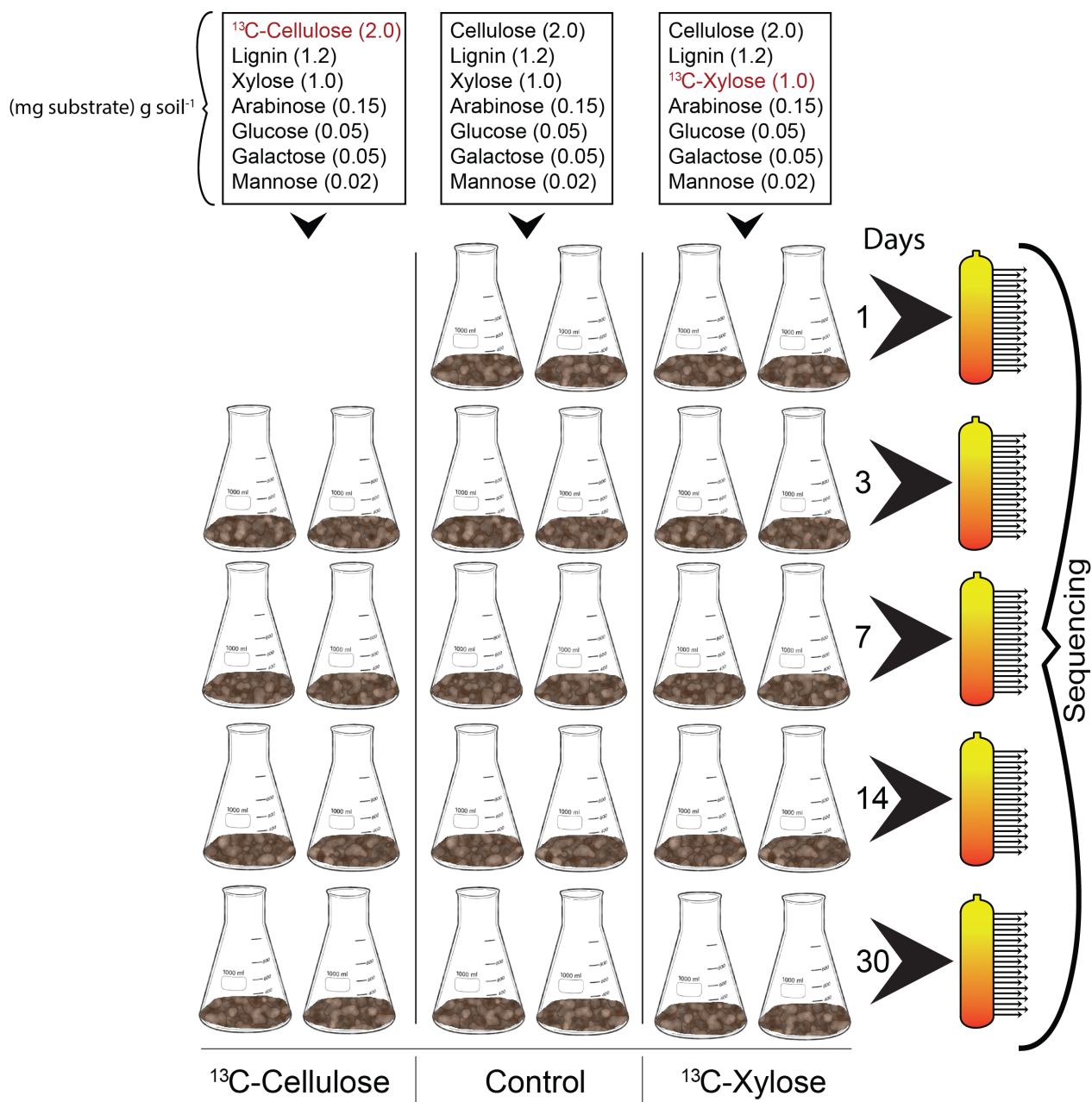


Fig. S1. The experimental design. A carbon mixture, in addition to inorganic salts and amino acids (not shown here), was added to each soil microcosm where the only difference between treatments is the ¹³C-labeled isotope (in red). At days 1, 3, 7, 14, and 30 replicate microcosms were destructively harvested for downstream molecular applications. Bulk DNA from each treatment and time point ($n = 14$) was CsCl density separated by centrifuged and fractionated (orange tubes wherein each arrow represents a fraction from the density gradient). Fractions were 16S gene sequenced using next generation sequencing technology.

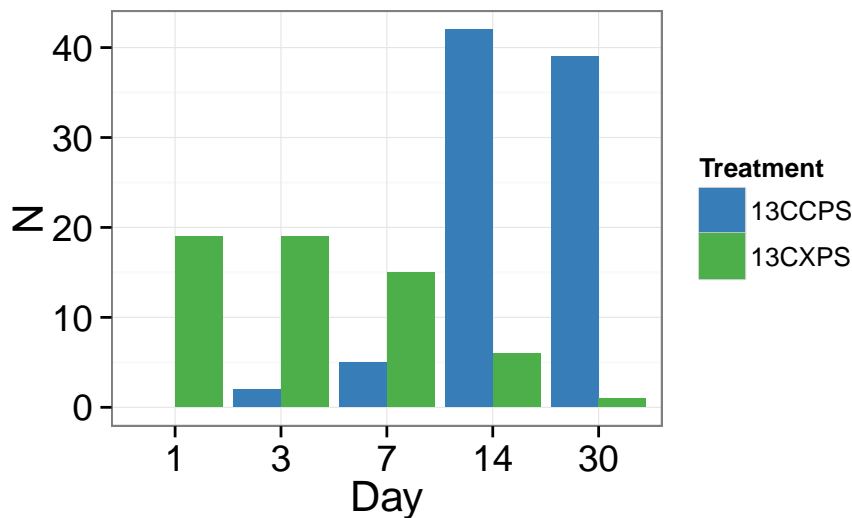


Fig. S2. Counts of responders to each isotopically labeled substrate (cellulose and xylose) over time.

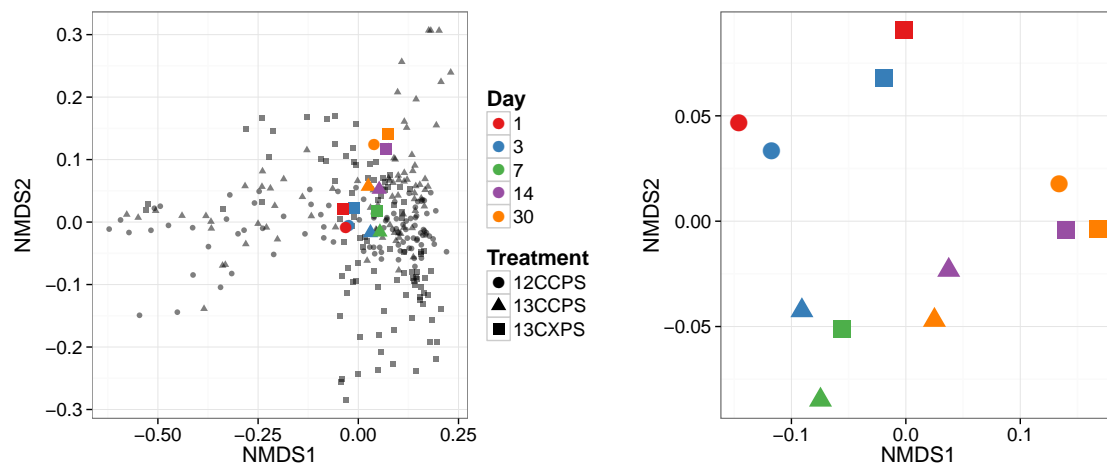


Fig. S3. Ordination of bulk gradient fraction phylogenetic profiles.

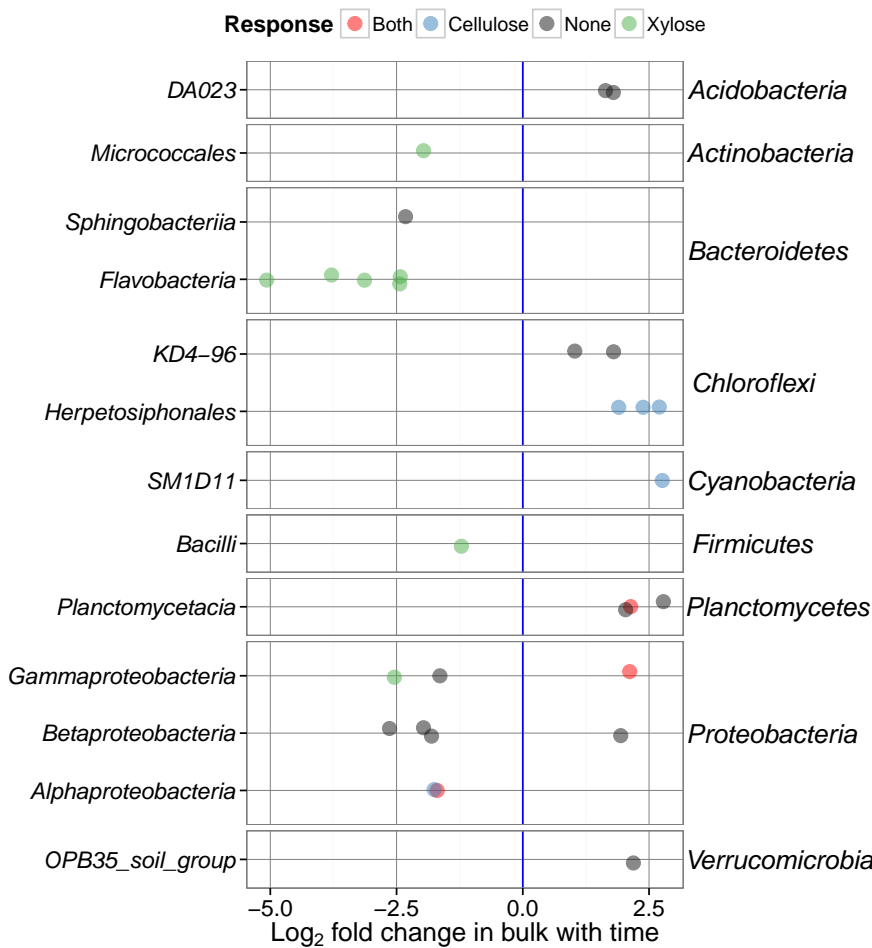


Fig. S4. Fold change time⁻¹ for OTUs that changed significantly in abundance over time. One panel per phylum (phyla indicated on the right). Taxonomic class indicated on the left.

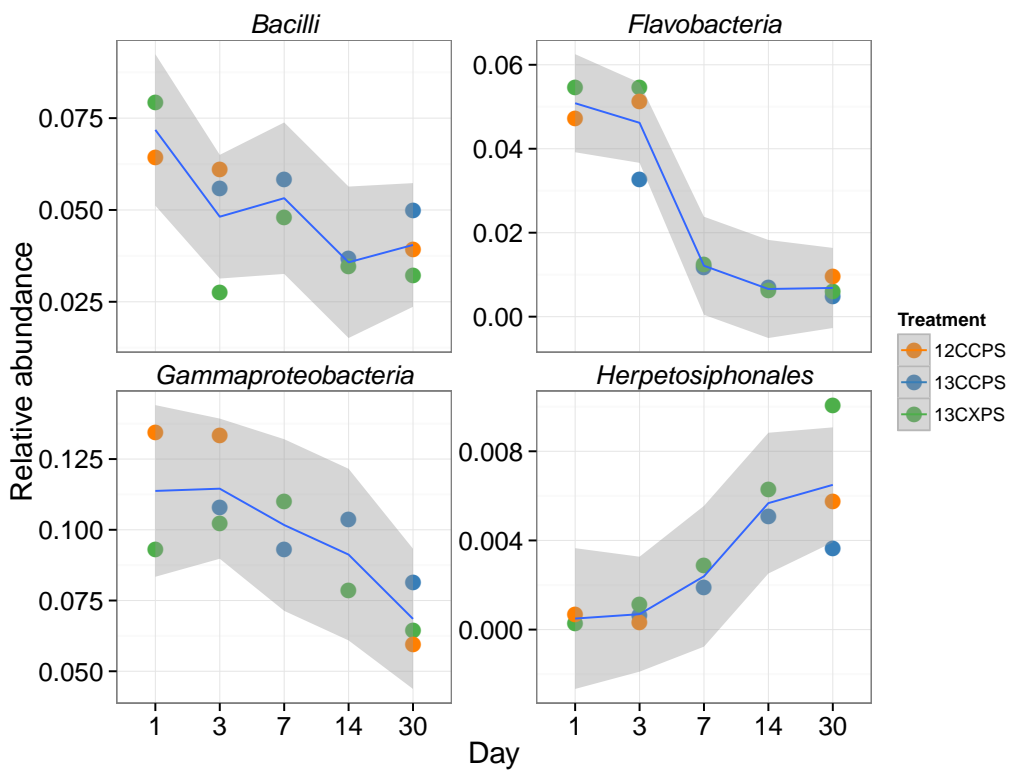
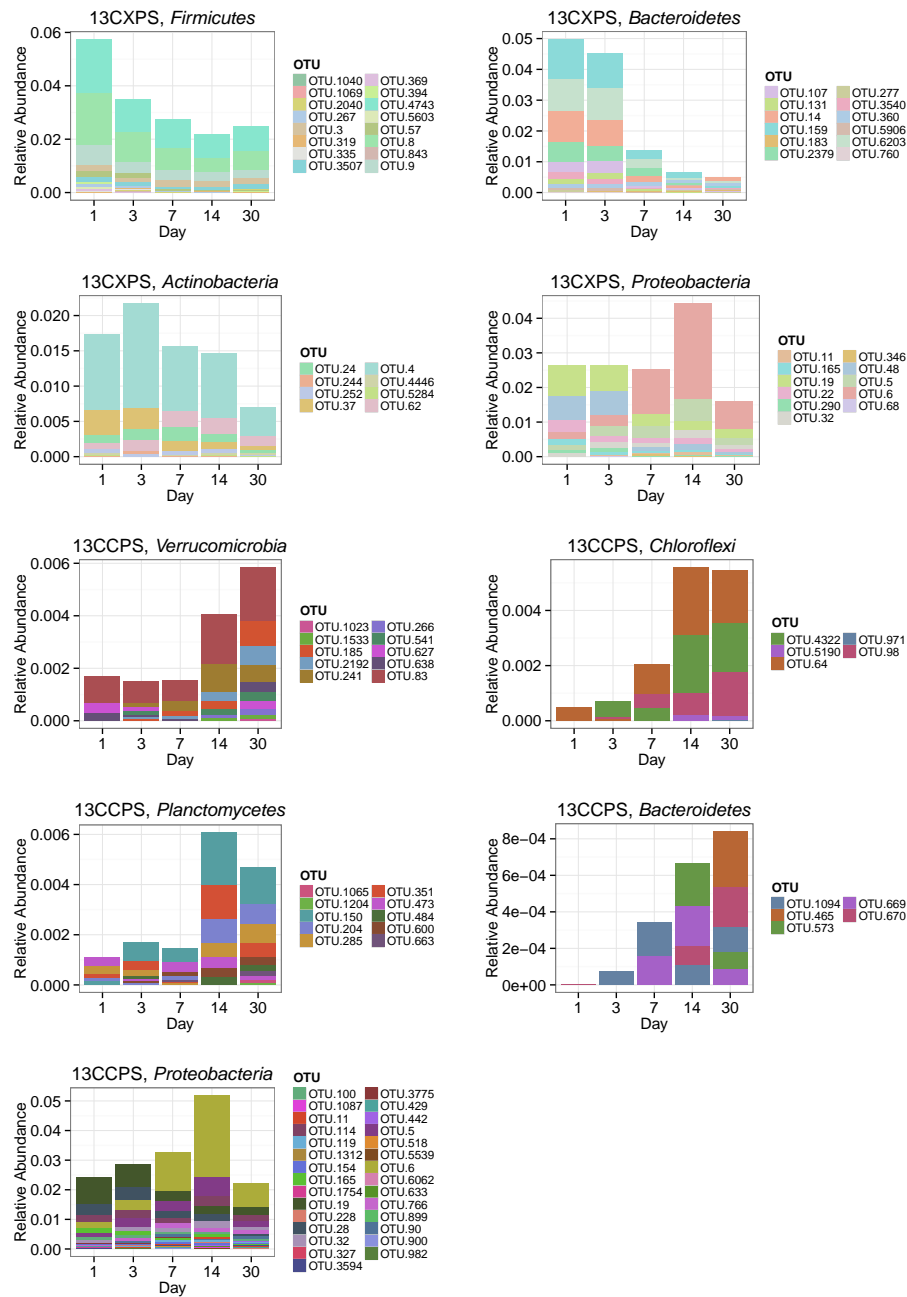


Fig. S5. Relative abundance versus day for classes that changed significantly in relative abundance with time.

**Fig. S6.** Sum of bulk abundances with selected phylum for responder OTUs.

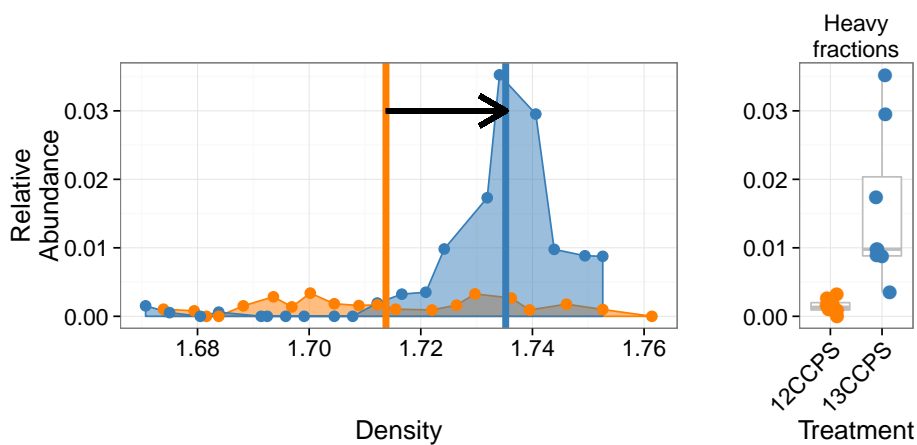


Fig. S7. Density profile for a single ^{13}C -cellulose “responder” OTU in the labeled gradient, blue, and the control gradient, orange. Vertical lines show center of mass for each density profile and arrow denotes the magnitude and direction of the BD shift upon labeling. Panel at right shows relative abundance values in the heavy fractions for each gradient.

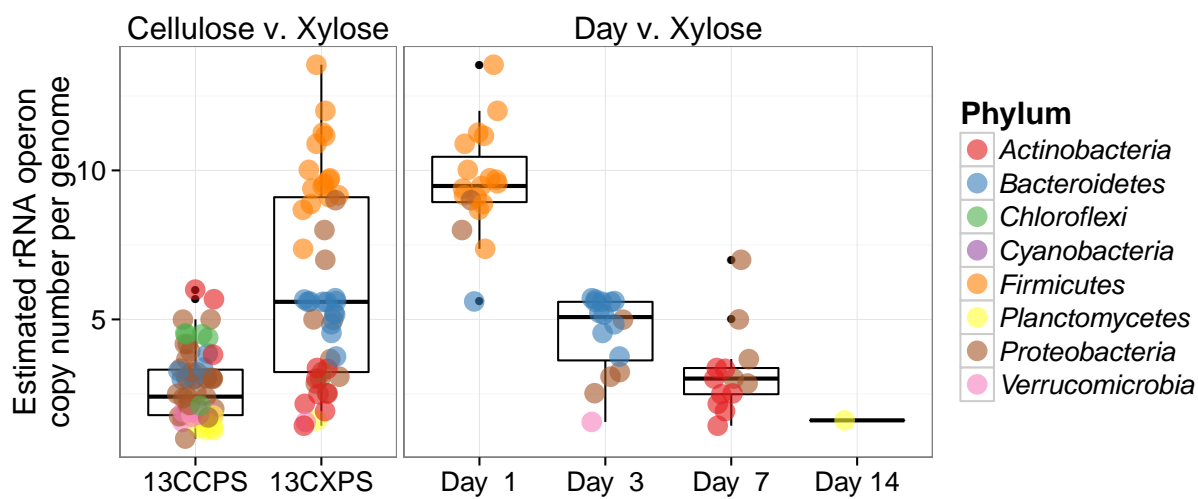


Fig. S8. Estimated rRNA operon copy number per genome for ^{13}C responding OTUs. Panel titles indicate which labeled substrate(s) are depicted.

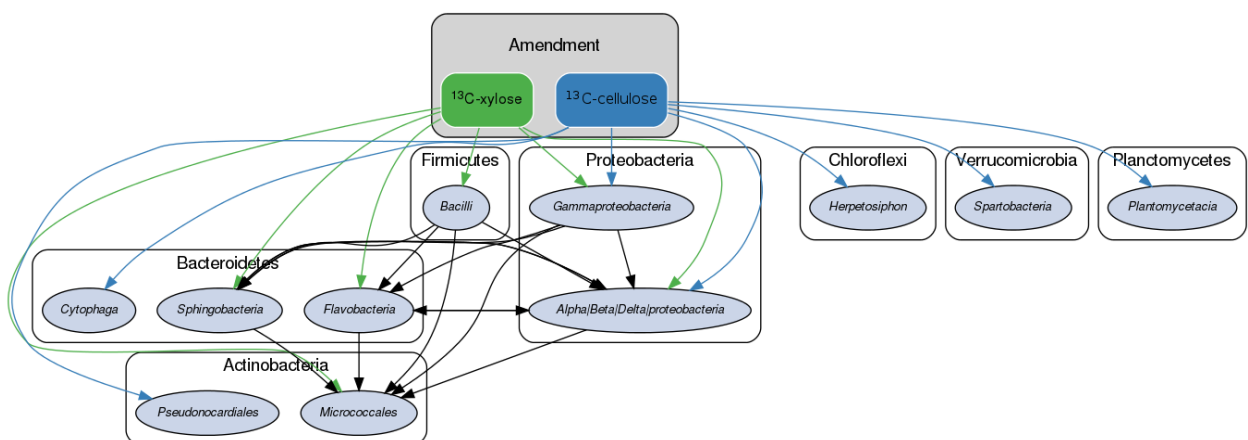


Fig. S9. Conceptual model of soil food web in this experiment. Taxa shown possessed at least two ¹³C responder OTUs for a given C substrate. *Proteobacteria* response was too varied taxonomically to depict at higher taxonomic resolution in this format. Black arrows indicate possible predator/prey interactions whereas colored arrows represent possible routes of primary degradation (green: xylose, blue: cellulose).

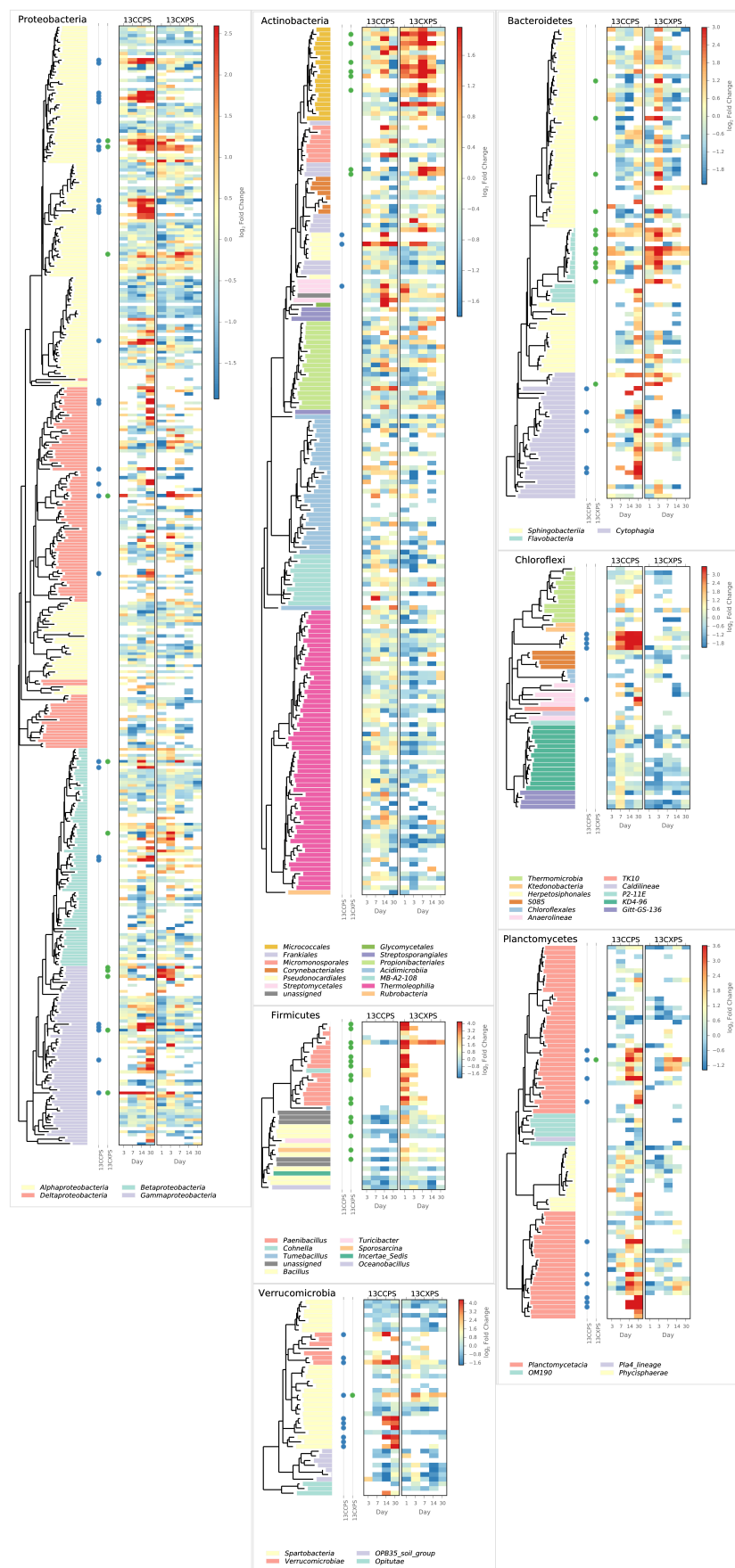


Fig. S10. Phylum specific trees. Heatmap indicates fold change between heavy fractions of control gradients versus labeled gradients. Dots indicate the position of “responders” to ^{13}C -xylose (green) or ^{13}C -cellulose (blue).

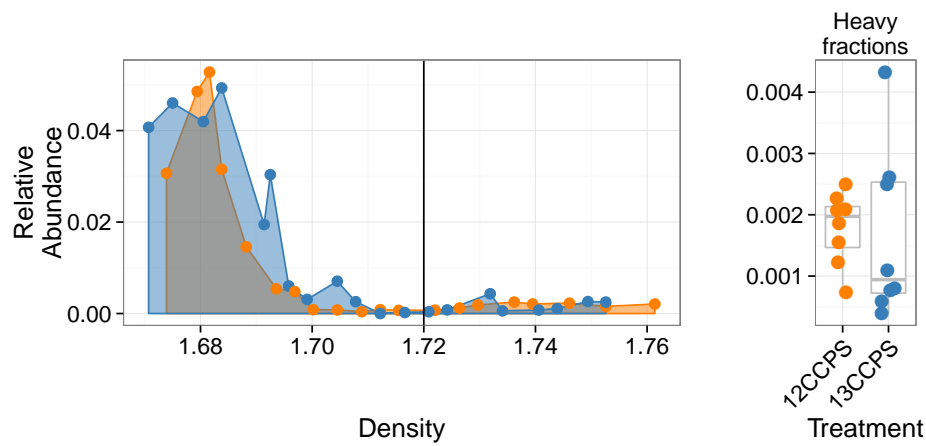


Fig. S11. Density profile for a single ^{13}C -cellulose "non-responder" OTU in the labeled gradient, blue, and the control gradient, orange. Vertical line shows where "heavy" fractions begin as defined in our analysis. Panel at right shows relative abundance values in the heavy fractions for each gradient.

Table S1: ¹³C-cellulose responders BLAST against Living Tree Project

OTU ID	Fold change ^a	Day ^b	Top BLAST hits	BLAST %ID	Phylum;Class;Order
OTU.100	2.66	14	<i>Pseudoxanthomonas sacheonensis</i> , <i>Pseudoxanthomonas dokdonensis</i>	100.0	Proteobacteria Gammaproteobacteria Xanthomonadales
OTU.1023	4.61	30	No hits of at least 90% identity	80.54	Verrucomicrobia Spartobacteria Chthoniobacterales
OTU.1065	5.31	14	No hits of at least 90% identity	84.55	Planctomycetes Planctomycetacia Planctomycetales
OTU.1087	4.32	14	<i>Devsia soli</i> , <i>Devsia crocina</i> , <i>Devsia riboflavina</i>	99.09	Proteobacteria Alphaproteobacteria Rhizobiales
OTU.1094	3.69	30	<i>Sporocytophaga myxococcoides</i>	99.55	Bacteroidetes Cytophagia Cytophagales
OTU.11	3.41	14	<i>Stenotrophomonas pavanii</i> , <i>Stenotrophomonas maltophilia</i> , <i>Pseudomonas geniculata</i>	99.54	Proteobacteria Gammaproteobacteria Xanthomonadales
OTU.114	2.78	14	<i>Herbaspirillum sp. SUEMI03</i> , <i>Herbaspirillum sp. SUEMI10</i> , <i>Oxalicibacterium solurbis</i> , <i>Herminiumonas fonticola</i> , <i>Oxalicibacterium horti</i>	100.0	Proteobacteria Betaproteobacteria Burkholderiales
OTU.119	3.31	14	<i>Brevundimonas alba</i>	100.0	Proteobacteria Alphaproteobacteria Caulobacterales
OTU.120	4.76	14	<i>Vampirovibrio chlorellavorus</i>	94.52	Cyanobacteria SM1D11 uncultured-bacterium
OTU.1204	4.32	30	<i>Planctomyces limnophilus</i>	91.78	Planctomycetes Planctomycetacia Planctomycetales
OTU.1312	4.07	30	<i>Paucimonas lemoignei</i>	99.54	Proteobacteria Betaproteobacteria Burkholderiales
OTU.132	2.81	14	<i>Streptomyces spp.</i>	100.0	Actinobacteria Streptomycetales Streptomycetaceae
OTU.150	4.06	14	No hits of at least 90% identity	86.76	Planctomycetes Planctomycetacia Planctomycetales
OTU.1533	3.43	30	No hits of at least 90% identity	82.27	Verrucomicrobia Spartobacteria Chthoniobacterales
OTU.154	3.24	14	<i>Pseudoxanthomonas mexicana</i> , <i>Pseudoxanthomonas japonensis</i>	100.0	Proteobacteria Gammaproteobacteria Xanthomonadales
OTU.165	3.1	14	<i>Rhizobium skieniewicense</i> , <i>Rhizobium vignae</i> , <i>Rhizobium larrymoorei</i> , <i>Rhizobium alkalisolii</i> , <i>Rhizobium galegae</i> , <i>Rhizobium huautlense</i>	100.0	Proteobacteria Alphaproteobacteria Rhizobiales
OTU.1754	4.48	14	<i>Asticcacaulis biprosthecium</i> , <i>Asticcacaulis benevestitus</i>	96.8	Proteobacteria Alphaproteobacteria Caulobacterales
OTU.185	4.37	14	No hits of at least 90% identity	85.14	Verrucomicrobia Spartobacteria Chthoniobacterales
OTU.19	2.44	14	<i>Rhizobium alamii</i> , <i>Rhizobium mesosinicum</i> , <i>Rhizobium mongolense</i> , <i>Arthrobacter viscosus</i> , <i>Rhizobium sullae</i> , <i>Rhizobium yanglingense</i> , <i>Rhizobium loessense</i>	99.54	Proteobacteria Alphaproteobacteria Rhizobiales
OTU.204	3.81	14	No hits of at least 90% identity	nan	Planctomycetes Planctomycetacia Planctomycetales

Table S1 – continued from previous page

OTU ID	Fold change	Day	Top BLAST hits	BLAST %ID	Phylum;Class;Order
OTU.2192	3.49	30	No hits of at least 90% identity	83.56	Verrucomicrobia Spartobacteria Chthoniobacterales
OTU.228	2.54	30	<i>Sorangium cellulosum</i>	98.17	Proteobacteria Deltaproteobacteria Myxococcales
OTU.241	2.66	14	No hits of at least 90% identity	87.73	Verrucomicrobia Spartobacteria Chthoniobacterales
OTU.257	2.94	14	<i>Lentzea waywayandensis</i> , <i>Lentzea flaviverrucosa</i>	100.0	Actinobacteria Pseudonocardiales Pseudonocardiaceae
OTU.266	4.54	30	No hits of at least 90% identity	83.64	Verrucomicrobia Spartobacteria Chthoniobacterales
OTU.28	2.59	14	<i>Rhizobium giardinii</i> , <i>Rhizobium tubonense</i> , <i>Rhizobium tibeticum</i> , <i>Rhizobium mesoamericanum CCGE 501</i> , <i>Rhizobium herbae</i> , <i>Rhizobium endophyticum</i>	99.54	Proteobacteria Alphaproteobacteria Rhizobiales
OTU.285	3.55	30	<i>Blastopirellula marina</i>	90.87	Planctomycetes Planctomycetacia Planctomycetales
OTU.32	2.34	3	<i>Sandaracinus amylolyticus</i>	94.98	Proteobacteria Deltaproteobacteria Myxococcales
OTU.327	2.99	14	<i>Asticcacaulis biprosthecum</i> , <i>Asticcacaulis benevestitus</i>	98.63	Proteobacteria Alphaproteobacteria Caulobacterales
OTU.351	3.54	14	<i>Pirellula staleyi DSM 6068</i>	91.86	Planctomycetes Planctomycetacia Planctomycetales
OTU.3594	3.83	30	<i>Chondromyces robustus</i>	90.41	Proteobacteria Deltaproteobacteria Myxococcales
OTU.3775	3.88	14	<i>Devosia glacialis</i> , <i>Devosia chinhatensis</i> , <i>Devosia geojensis</i> , <i>Devosia yakushimensis</i>	98.63	Proteobacteria Alphaproteobacteria Rhizobiales
OTU.429	3.7	30	<i>Devosia limi</i> , <i>Devosia psychrophila</i>	97.72	Proteobacteria Alphaproteobacteria Rhizobiales
OTU.4322	4.19	14	No hits of at least 90% identity	89.14	Chloroflexi Herpetosiphonales Herpetosiphonaceae
OTU.442	3.05	30	<i>Chondromyces robustus</i>	92.24	Proteobacteria Deltaproteobacteria Myxococcales
OTU.465	3.79	30	<i>Ohtaekwangia kribbensis</i>	92.73	Bacteroidetes Cytophagia Cytophagales
OTU.473	3.58	14	<i>Pirellula staleyi DSM 6068</i>	90.91	Planctomycetes Planctomycetacia Planctomycetales
OTU.484	4.92	14	No hits of at least 90% identity	89.09	Planctomycetes Planctomycetacia Planctomycetales
OTU.5	2.69	14	<i>Delftia tsuruhatensis</i> , <i>Delftia lacustris</i>	100.0	Proteobacteria Betaproteobacteria Burkholderiales
OTU.518	4.8	14	<i>Hydrogenophaga intermedia</i>	100.0	Proteobacteria Betaproteobacteria Burkholderiales
OTU.5190	3.6	30	No hits of at least 90% identity	88.13	Chloroflexi Herpetosiphonales Herpetosiphonaceae
OTU.541	4.49	30	No hits of at least 90% identity	84.23	Verrucomicrobia Spartobacteria Chthoniobacterales
OTU.5539	4.01	14	<i>Devosia subaequoris</i>	98.17	Proteobacteria Alphaproteobacteria Rhizobiales

Table S1 – continued from previous page

OTU ID	Fold change	Day	Top BLAST hits	BLAST %ID	Phylum;Class;Order
OTU.573	3.03	30	<i>Adhaeribacter aerophilus</i>	92.76	<i>Bacteroidetes Cytophagia Cytophagales</i>
OTU.6	3.62	7	<i>Cellvibrio fulvus</i>	100.0	<i>Proteobacteria Gammaproteobacteria Pseudomonadales</i>
OTU.600	3.48	30	No hits of at least 90% identity	80.37	<i>Planctomycetes Planctomycetacia Planctomycetales</i>
OTU.6062	4.83	30	<i>Dokdonella sp. DC-3, Luteibacter rhizovicinus</i>	97.26	<i>Proteobacteria Gammaproteobacteria Xanthomonadales</i>
OTU.627	4.43	14	<i>Verrucomicrobiaceae bacterium DC2a-G7</i>	100.0	<i>Verrucomicrobia Verrucomicrobiae Verrucomicrobiales</i>
OTU.633	3.84	30	No hits of at least 90% identity	89.5	<i>Proteobacteria Deltaproteobacteria Myxococcales</i>
OTU.638	4.0	30	<i>Luteolibacter sp. CCTCC AB 2010415, Luteolibacter algae</i>	93.61	<i>Verrucomicrobia Verrucomicrobiae Verrucomicrobiales</i>
OTU.64	4.31	14	No hits of at least 90% identity	89.5	<i>Chloroflexi Herpetosiphonales Herpetosiphonaceae</i>
OTU.663	3.63	30	<i>Pirellula staleyi DSM 6068</i>	90.87	<i>Planctomycetes Planctomycetacia Planctomycetales</i>
OTU.669	3.34	30	<i>Ohtaekwangia koreensis</i>	92.69	<i>Bacteroidetes Cytophagia Cytophagales</i>
OTU.670	2.87	30	<i>Adhaeribacter aerophilus</i>	91.78	<i>Bacteroidetes Cytophagia Cytophagales</i>
OTU.766	3.21	14	<i>Devosia insulae</i>	99.54	<i>Proteobacteria Alphaproteobacteria Rhizobiales</i>
OTU.83	5.61	14	<i>Luteolibacter sp. CCTCC AB 2010415</i>	97.72	<i>Verrucomicrobia Verrucomicrobiae Verrucomicrobiales</i>
OTU.862	5.87	14	<i>Allokutzneria albata</i>	100.0	<i>Actinobacteria Pseudonocardiales Pseudonocardiaceae</i>
OTU.899	2.28	30	<i>Enhygromyxa salina</i>	97.72	<i>Proteobacteria Deltaproteobacteria Myxococcales</i>
OTU.90	2.94	14	<i>Sphingopyxis panaciterrae, Sphingopyxis chilensis, Sphingopyxis sp. BZ30, Sphingomonas sp.</i>	100.0	<i>Proteobacteria Alphaproteobacteria Sphingomonadales</i>
OTU.900	4.87	14	<i>Brevundimonas vesicularis, Brevundimonas nasdae</i>	100.0	<i>Proteobacteria Alphaproteobacteria Caulobacterales</i>
OTU.971	3.68	30	No hits of at least 90% identity	78.57	<i>Chloroflexi Anaerolineae Anaerolineales</i>
OTU.98	3.68	14	No hits of at least 90% identity	88.18	<i>Chloroflexi Herpetosiphonales Herpetosiphonaceae</i>
OTU.982	4.47	14	<i>Devosia neptuniae</i>	100.0	<i>Proteobacteria Alphaproteobacteria Rhizobiales</i>

^a Maximum observed \log_2 of fold change.^b Day of maximum fold change.

Table S2: ¹³C-xylose responders BLAST against Living Tree Project

OTU ID	Fold change ^a	Day ^b	Top BLAST hits	BLAST %ID	Phylum;Class;Order
OTU.1040	4.78	1	<i>Paenibacillus daejeonensis</i>	100.0	<i>Firmicutes Bacilli Bacillales</i>
OTU.1069	3.85	1	<i>Paenibacillus terrigena</i>	100.0	<i>Firmicutes Bacilli Bacillales</i>
OTU.107	2.25	3	<i>Flavobacterium sp. 15C3</i> , <i>Flavobacterium banpakuense</i>	99.54	<i>Bacteroidetes Flavobacteria Flavobacteriales</i>
OTU.11	5.25	7	<i>Stenotrophomonas pavanii</i> , <i>Stenotrophomonas maltophilia</i> , <i>Pseudomonas geniculata</i>	99.54	<i>Proteobacteria Gammaproteobacteria Xanthomonadales</i>
OTU.131	3.07	3	<i>Flavobacterium fluvii</i> , <i>Flavobacterium bacterium HMD1033</i> , <i>Flavobacterium sp. HMD1001</i>	100.0	<i>Bacteroidetes Flavobacteria Flavobacteriales</i>
OTU.14	3.92	3	<i>Flavobacterium oncorhynchi</i> , <i>Flavobacterium glycines</i> , <i>Flavobacterium succinicans</i>	99.09	<i>Bacteroidetes Flavobacteria Flavobacteriales</i>
OTU.150	3.08	14	No hits of at least 90% identity	86.76	<i>Planctomycetes Planctomycetacia Planctomycetales</i>
OTU.159	3.16	3	<i>Flavobacterium hibernum</i>	98.17	<i>Bacteroidetes Flavobacteria Flavobacteriales</i>
OTU.165	2.38	3	<i>Rhizobium skieniewicense</i> , <i>Rhizobium vignae</i> , <i>Rhizobium larrymoorei</i> , <i>Rhizobium alkalisolii</i> , <i>Rhizobium galegae</i> , <i>Rhizobium huautlense</i>	100.0	<i>Proteobacteria Alphaproteobacteria Rhizobiales</i>
OTU.183	3.31	3	No hits of at least 90% identity	89.5	<i>Bacteroidetes Sphingobacteriia Sphingobacteriales</i>
OTU.19	2.14	7	<i>Rhizobium alamii</i> , <i>Rhizobium mesosinicum</i> , <i>Rhizobium mongolense</i> , <i>Arthrobacter viscosus</i> , <i>Rhizobium sullae</i> , <i>Rhizobium yanglingense</i> , <i>Rhizobium loessense</i>	99.54	<i>Proteobacteria Alphaproteobacteria Rhizobiales</i>
OTU.2040	2.91	1	<i>Paenibacillus pectinilyticus</i>	100.0	<i>Firmicutes Bacilli Bacillales</i>
OTU.22	2.8	7	<i>Paracoccus sp. NB88</i>	99.09	<i>Proteobacteria Alphaproteobacteria Rhodobacterales</i>
OTU.2379	3.1	3	<i>Flavobacterium pectinovorum</i> , <i>Flavobacterium sp. CS100</i>	97.72	<i>Bacteroidetes Flavobacteria Flavobacteriales</i>
OTU.24	2.81	7	<i>Cellulomonas aerilata</i> , <i>Cellulomonas humilata</i> , <i>Cellulomonas terrae</i> , <i>Cellulomonas soli</i> , <i>Cellulomonas xylinilytica</i>	100.0	<i>Actinobacteria Micrococcales Cellulomonadaceae</i>
OTU.241	3.38	3	No hits of at least 90% identity	87.73	<i>Verrucomicrobia Spartobacteria Chthoniobacterales</i>
OTU.244	3.08	7	<i>Cellulosimicrobium funkei</i> , <i>Cellulosimicrobium terreum</i>	100.0	<i>Actinobacteria Micrococcales Promicromonosporaceae</i>
OTU.252	3.34	7	<i>Promicromonospora thailandica</i>	100.0	<i>Actinobacteria Micrococcales Promicromonosporaceae</i>
OTU.267	4.97	1	<i>Paenibacillus pabuli</i> , <i>Paenibacillus tundrae</i> , <i>Paenibacillus taichungensis</i> , <i>Paenibacillus xylohexedens</i> , <i>Paenibacillus xylinilyticus</i>	100.0	<i>Firmicutes Bacilli Bacillales</i>
OTU.277	3.52	3	<i>Solibius ginsengiterrae</i>	95.43	<i>Bacteroidetes Sphingobacteriia Sphingobacteriales</i>

Table S2 – continued from previous page

OTU ID	Fold change	Day	Top BLAST hits	BLAST %ID	Phylum;Class;Order
OTU.290	3.59	1	<i>Pantoea spp.</i> , <i>Klugvera spp.</i> , <i>Klebsiella spp.</i> , <i>Erwinia spp.</i> , <i>Enterobacter spp.</i> , <i>Buttiauxella spp.</i>	100.0	Proteobacteria Gammaproteobacteria Enterobacterales
OTU.3	2.61	1	[<i>Brevibacterium</i>] <i>frigoritolerans</i> , <i>Bacillus sp. LMG 20238</i> , <i>Bacillus coahuilensis m4-4</i> , <i>Bacillus simplex</i>	100.0	Firmicutes Bacilli Bacillales
OTU.319	3.98	1	<i>Paenibacillus xinjiangensis</i>	97.25	Firmicutes Bacilli Bacillales
OTU.32	3.0	3	<i>Sandaracinus amyloyticus</i>	94.98	Proteobacteria Deltaproteobacteria Myxococcales
OTU.335	2.53	1	<i>Paenibacillus thailandensis</i>	98.17	Firmicutes Bacilli Bacillales
OTU.346	3.44	3	<i>Pseudoduganella violaceinigra</i>	99.54	Proteobacteria Betaproteobacteria Burkholderiales
OTU.3507	2.36	1	<i>Bacillus spp.</i>	98.63	Firmicutes Bacilli Bacillales
OTU.3540	2.52	3	<i>Flavobacterium terrigena</i>	99.54	Bacteroidetes Flavobacteria Flavobacterales
OTU.360	2.98	3	<i>Flavisolibacter ginsengisoli</i>	95.0	Bacteroidetes Sphingobacteriia Sphingobacterales
OTU.369	5.05	1	<i>Paenibacillus sp. D75</i> , <i>Paenibacillus glycansilyticus</i>	100.0	Firmicutes Bacilli Bacillales
OTU.37	2.68	7	<i>Phycicola gilvus</i> , <i>Microterricola viridarii</i> , <i>Frigeribacterium faeni</i> , <i>Frondihabitans sp. RS-15</i> , <i>Frondihabitans australicus</i>	100.0	Actinobacteria Micrococcales Microbacteriaceae
OTU.394	4.06	1	<i>Paenibacillus pocheonensis</i>	100.0	Firmicutes Bacilli Bacillales
OTU.4	2.84	7	<i>Agromyces ramosus</i>	100.0	Actinobacteria Micrococcales Microbacteriaceae
OTU.4446	3.49	7	<i>Catenuloplanes niger</i> , <i>Catenuloplanes castaneus</i> , <i>Catenuloplanes atrovinosus</i> , <i>Catenuloplanes crispus</i> , <i>Catenuloplanes nepalensis</i> , <i>Catenuloplanes japonicus</i>	97.72	Actinobacteria Frankiales Nakamurellaceae
OTU.4743	2.24	1	<i>Lysinibacillus fusiformis</i> , <i>Lysinibacillus sphaericus</i>	99.09	Firmicutes Bacilli Bacillales
OTU.48	2.99	1	<i>Aeromonas spp.</i>	100.0	Proteobacteria Gammaproteobacteria aaa34a10
OTU.5	3.69	7	<i>Delftia tsuruhatensis</i> , <i>Delftia lacustris</i>	100.0	Proteobacteria Betaproteobacteria Burkholderiales
OTU.5284	3.56	7	<i>Isoptericola nanjingensis</i> , <i>Isoptericola hypogaeus</i> , <i>Isoptericola variabilis</i>	98.63	Actinobacteria Micrococcales Promicromonosporaceae
OTU.5603	3.96	1	<i>Paenibacillus uliginis</i>	100.0	Firmicutes Bacilli Bacillales
OTU.57	4.39	1	<i>Paenibacillus castaneae</i>	98.62	Firmicutes Bacilli Bacillales
OTU.5906	3.16	3	<i>Terrimonas sp. M-8</i>	96.8	Bacteroidetes Sphingobacteriia Sphingobacterales
OTU.6	3.24	3	<i>Cellvibrio fulvus</i>	100.0	Proteobacteria Gammaproteobacteria Pseudomonadales
OTU.62	2.57	7	<i>Nakamurella flava</i>	100.0	Actinobacteria Frankiales Nakamurellaceae

Table S2 – continued from previous page

OTU ID	Fold change	Day	Top BLAST hits	BLAST %ID	Phylum;Class;Order
OTU.6203	3.32	3	<i>Flavobacterium granuli</i> , <i>Flavobacterium glaciei</i>	100.0	<i>Bacteroidetes Flavobacteria Flavobacteriales</i>
OTU.68	3.74	7	<i>Shigella flexneri</i> , <i>Escherichia fergusonii</i> , <i>Escherichia coli</i> , <i>Shigella sonnei</i>	100.0	<i>Proteobacteria Gammaproteobacteria Enterobacteriales</i>
OTU.760	2.89	3	<i>Dyadobacter hamtensis</i>	98.63	<i>Bacteroidetes Cytophagia Cytophagales</i>
OTU.8	2.26	1	<i>Bacillus niaci</i>	100.0	<i>Firmicutes Bacilli Bacillales</i>
OTU.843	3.62	1	<i>Paenibacillus agaragedens</i>	100.0	<i>Firmicutes Bacilli Bacillales</i>
OTU.9	2.04	1	<i>Bacillus megaterium</i> , <i>Bacillus flexus</i>	100.0	<i>Firmicutes Bacilli Bacillales</i>

^a Maximum observed \log_2 of fold change.^b Day of maximum fold change.